A Methodology for Evaluating UAM Noise and Visual Pollution

M. Baena, M. Alonso, D. Mocholí
Nommon Solutions and Technologies
Madrid, Spain

C. Barrado
UPC
Barcelona, Spain

I. LeGriffon, E. Ruaud
ONERA
Paris, France

E. Ganić, T. Krstić Simić
University of Belgrade
Belgrade, Serbia

***Abstract*—This paper proposes an innovative methodology to evaluate the noise and visual pollution generated by UAM activities, with a particular focus on how these impacts vary across different population segments (e.g., differentiating by age and gender). We present the outcomes of a novel simulation toolset that models drone-generated noise and visual pollution, integrating these data with dynamic population distribution maps derived from the combination of mobile network data and GPS data from personal mobile devices. The analysis focuses on three case studies in the city of Madrid: the impact of a drone flying over residential and downtown areas during the cruise phase; the effects of take-off in a residential neighbourhood; and the cumulative effects of multiple flights. These results offer valuable insights into the local environmental impacts of UAM and are expected to contribute to the development of more targeted U-space regulations and social acceptance strategies.**

Keywords-UAM, environment, visual pollution, noise, mobile network data

I. INTRODUCTION

The development of U-space is crucial for enabling urban air mobility (UAM) and unlocking the drone economy, offering benefits such as enhanced medical transport, goods delivery, and job creation. However, relevant challenges are still to be solved, particularly regarding drone operations over densely populated areas. The European Union Aviation Safety Agency (EASA) has conducted a comprehensive study on the societal acceptance of UAM across the EU [1]. When asking EU citizens about their concerns regarding UAM operations, safety and noise come first, but the range of concerns is much broader and includes other impacts such as visual pollution, induced stress due to traffic movements above one's head, security, privacy, and the occupation by take-off and landing facilities of urban spaces that would be better used for living or recreation.

The efforts to characterise and quantify UAM's impact on the quality of public spaces are still scarce [2], mainly assessing public perception on UAM through surveys and questionnaires [3]. The SESAR 2020 PJ19.04 project has begun to develop indicators to assess UAM's environmental impact [4], but these indicators are still too broad to capture UAM's diverse effects on different urban contexts. Noise and visual pollution are the two most addressed negative effects, related to the implementation of UAVs and eVTOLs as part of UAM [5]. More advanced tools are needed to understand the interaction between UAM operations, environmental impacts, and citizens' use of public spaces. For example, using census data implies the unrealistic assumption that people spend 24 hours at their residence area and ignores the dynamics of daytime activity, including routine travel and more occasional trips to perform activities at different locations, overlooking the fact that some residents spend a long time far from the area which is supposed to represent their exposure, which can lead to significant biases in the estimation of exposure [6].

The MUSE project [7] aims to address this gap by creating a set of performance indicators (PIs), methods, and tools to assess UAM's social and environmental impacts on urban life, which are expected to serve as an enabler of a future U-space service aimed at optimising the social and environmental performance of UAM operations. This paper presents the methodology developed by MUSE for measuring the environmental impact of UAM, detailing the models and workflow used. The methodology is demonstrated and evaluated through two test scenarios in the city of Madrid. The first scenario compares the impact of drone flights during the cruise phase over residential and downtown areas, while the second evaluates the effects of take-off operations in a residential neighbourhood.

The rest of the paper is structured as follows: Section II describes the methodology followed to assess the environmental impact of UAM, describing its main steps (trajectory generation, noise modelling, visual pollution modelling, dynamic population mapping and population exposure and indicators calculation), Section III describes the case studies analysed in the paper in Section IV, which provides the results analysed in the paper, and finally Section V provides the conclusions.

II. METHODOLOGY

The methodology designed to assess the environmental impact of UAM operations is illustrated in Fig. 1. This approach consists of the following sequentially connected modules: (i) trajectory generation, to accurately model 4D drone trajectories in urban areas in the absence of historical trajectory data; (ii) noise modelling, to assess noise emissions along these trajectories and their propagation across various parts of the city; (iii) visual pollution modelling, to evaluate the visual impact of the trajectories; (iv) dynamic population mapping, to track the spatial distribution of the population at any given time; and (v) population exposure and indicator calculation, which involves modelling population exposure by integrating population distributions with noise and visual footprints and calculating PIs.

A. Trajectory generation

In the absence of real drone traffic over cities, it is necessary to recreate realistic trajectories to assess their environmental impact. To achieve this, we use GEMMA, a trajectory generation engine developed by the Technical University of Catalonia, which is designed to create realistic flight missions in various environments, ranging from simple point-to-point flights to complex operations such as scans and loitering. The software is highly configurable, enabling users to incorporate various operational layers, including flight schemes (e.g., visual line of sight, extended line of sight, beyond line of sight), airspace restrictions (e.g., no-fly zones, flight altitudes, geofencing), performance data of the aircraft in the operator's fleet, operator types, and geographical settings. GEMMA has been utilised to validate urban air mobility capacity limits and test strategic conflict detection services [8]. The trajectory generation leverages drones' performances obtained from the BlueSky simulator [9] to define the speed and city 3D models for determining flight altitude with respect to terrain and obstacles.

B. Noise modelling

The noise module consists of three integrated tools: (i) DynaPyVTOL for flight mechanics, (ii) CARMEN for noise source calculation, and (iii) NoiseModelling for noise propagation. DynaPyVTOL and CARMEN are proprietary tools developed by ONERA, while NoiseModelling is open-source software.

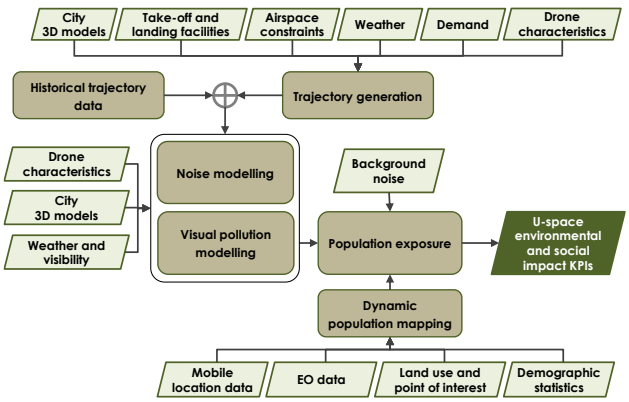

Figure 1. Methodology workflow.

These tools are used sequentially. First, DynaPyVTOL processes data from the trajectory generation engine (GEMMA), providing dynamic information on vehicle and propeller behaviour, including flight trajectory, 3D vehicle orientation, and parameters such as propeller thrust, torque, and RPM. This data is then fed into CARMEN, which calculates noise emissions at each time step, represented as emission spheres [10][11]. Finally, NoiseModelling aggregates these noise emissions, calculates their propagation in accordance with CNOSSOS-EU directives [12] for rail and road noise, and applies advanced ray-tracing methods [13], to generate noise maps. These maps provide relevant metrics for computing noise-related indicators.

C. Visual pollution modelling

Visual pollution is the compounded effect of disorder and excess of various objects in a landscape which population finds unattractive, ugly, intrusive or disturbing [14][15]. In order to calculate it, this module leverages standard GIS software functionalities to analyse landscape visibility using raster data, combined with geometric analysis of drone visibility from the ground along their flight paths. The raster data used, specifically the Digital Surface Model (DSM), includes terrain elevations as well as buildings and other structures that affect visibility. Trajectory and drone size data are incorporated to determine the areas where drones are observable and assess the visual impact on citizens.

To quantify visual pollution, we use the visual pollution concentration (VPC), a metric that assesses the intensity or density of visual pollution in a given area. Two methods are explored to calculate the VPC:

- AirMOUR: the visual pollution concentration is calculated based on the formula derived by the project AirMOUR [5]:

$$VPC = 47.76\,\frac{N^{0.65}}{D^{0.67}} + 1.37, \qquad (1)$$

  where N is the number of unmanned aircraft (UAs) visible by the observer, and D represents the distance from the observer to the closest UA. This formula estimates the intensity of visual pollution based on the number and proximity of UAs, but neglecting their size.

- Visual area: the visual area occupied by the drone is compared to the observer's visible field of view that is free of urban objects (i.e., open sky). This approach considers both the drone's dimensions (width and length) and its distance from the observer. The area occupied by the drone, Ω(drone), is calculated using trigonometric formulas that take into account the distance at which the drone is, R, its width and length for an estimation of the area (a). Then, the visual pollution concentration is defined as

$$VPC = CF\,\frac{\sum_i^N \Omega(drone_i)}{\Omega(open\ sky)} = CF\,\frac{\sum_i^N \tan^{-1}(a_i/R_i^2)}{4\pi - \Omega(urban)}. \qquad (2)$$

This metric is normalised considering the visible area occupied by a drone with $1m^2$ area located at 100m from the observer and the solid angle of open sky with no buildings (2π), i.e., $CF = 2\pi / \tan^{-1}(1/100^2)$.

D. Population mapping

The analysis of population exposure to UAM noise and visual pollution requires precise, detailed information on the population's presence across the city at different times. To obtain this information, this module leverages anonymised mobile network data (MND). MND are processed using Nommon's Population Insights software [16], a state-of-the-art platform that processes MND and integrates it with additional data layers (e.g., land use, points of interest, transport networks, and sociodemographic statistics) to create dynamic population maps, floating population statistics, and customisable presence and activity indicators. These indicators can be segmented by factors such as sociodemographic profile, activity type (e.g., home, work, education, pass-through traffic), length of stay, and visit frequency.

However, MND has limitations in terms of geographical resolution, and both noise and visual pollution impacts vary significantly with distance, requiring much finer resolution. To address this, we combined the information extracted from MND with GPS data from mobile apps to allocate people into smaller areas, following the approach proposed in [17]. The process uses historical GPS data to calculate the probability of individuals being present in different parts of a square grid at various times of the day. This probability heat map is then applied to the total number of people estimated from MND, achieving a resolution of a 15-meter grid.

E. Exposure and indicators calculation

The noise and visual pollution maps calculated are merged with population presence, segmented by sociodemographic profiles, to capture the interplay between the UAM's concept of operations (e.g., geofencing, route design, allowed traffic density), drones' visual and noise footprint, and citizens' spatial behaviour and use of public space.

The specific calculations vary depending on the indicators to be computed. In this paper, we present the results for the following indicators, included in the MUSE U-space Environmental and Social Performance Framework D3.1 [18].

TABLE I. PERFORMANCE INDICATORS

PIs	Unit	Measurement mechanism
NO-1: Area based people exposure to noise (L_Aeq)	person	The amount of people exposed to an equivalent noise level higher than a certain threshold in dBA[a], for a fixed period of time, within an area.
NO-2: Area based people exposure to Day-evening-night noise level (L_DEN)	person	The amount of people exposed to day-evening-night noise level (L_DEN) higher than a certain threshold in dBA, over a whole day (24 hours), within an area.
NO-5: Area based people exposure duration to noise	D.person	A certain duration D of noise levels exceeding a certain threshold in dBA multiplied by the number of people exposed, over a fixed period of time, within an area.
VP-1: Trajectory-based people exposed	person	The amount of people exposed to a single drone operation, i.e., sum of individual persons that are able to see the drone.
VP-2: Trajectory-based people exposed by concentration threshold	person	The amount of people exposed to a visual pollution concentration higher than a threshold, for a single drone operation.
VP-4: Trajectory based visual exposure	person.vp.h	Total visual pollution exposure perceived by the people exposed to a single drone operation.

a. dBA, are decibel scale readings that have been adjusted in an attempt to take into account the varying sensitivity of the human ear to different frequencies of sound.

III. CASE STUDIES

The proposed methodology has been evaluated using a series of test case studies with the aim of assessing its usefulness to evaluate the environmental impact of different types of UAM operations. For this purpose, three different cases, all located in Madrid, have been considered:

- Cruise flight: the impact of a single drone flying over a defined area has been analysed. The cruise flight takes place in the city centre of Madrid, from South to North, crossing residential, commercial, and downtown areas with a high density of pedestrians. The study focuses on an area around the congested Gran Via street and Puerta del Sol square. The cruise altitude is set at 105 meters above the elevation of the destination hospital rooftop, which stands at 704 meters in the ETRS89 reference. The indicators discussed for this case are: NO5, VP1, VP2, and VP4, see TABLE I.
- Take-off flight: the impact of a single drone during take-off from a specific vertiport has been assessed. The take-off flight is located in the residential district of Arganzuela. The mission starts at 13 meters above the ground and climbs to 200 meters during this phase, while adjusting its trajectory. The indicators discussed for this case are: NO1, VP1, and VP4.
- Traffic: the impact of multiple flights taking off and flying over the defined area throughout a study day has been analysed. Specifically, we consider six flights with the same origin and destination as the cruise flight previously presented, distributed throughout the day, and one take-off flight similar to the previous case. This case was considered to represent the NO2 indicator, which specifically addresses the combined effects of noise during the day, evening, and night.

For all these cases, MND and GPS data have been used to precisely map the population exposed to the considered UAM operations. MND data from March 2017 was used. To train the

population distribution algorithms that refine the precision of the MND data, we used GPS data from February, July, August, October, and November 2023, as well as from January, April, and May 2024. It is important to note that larger time periods are required for GPS data due to the fact that the sample size is significantly smaller than that provided by MND.

IV. RESULTS

This section presents the results of the PIs calculated for each of the test case studies analysed. The noise results provided here are illustrative rather than final, as their primary purpose is to validate the correct operation of the toolset and the integration of its individual components. More accurate drone noise models will be used in subsequent stages of the project to refine these results.

A. Cruise flight

1) Noise

Fig. 2 shows, in different colours, the duration (in seconds) of noise exceeding a theoretical 5 dB threshold produced during the cruise flight of a single drone. This map enables the calculation of the duration of people's exposure to noise in specific areas (NO5). The map illustrates the aggregation of noise produced along the drone's flight path. As expected, the effect diminishes with increasing distance from the drone's trajectory.

Fig. 3 shows the results for the NO5 indicator, which weights the previous noise map with the population presence data. TABLE II. presents the results disaggregated by gender and age. While there are no significant differences in the impact on men and women, a notable insight from the data is the disparity between the impact on age groups 25-44 and 45-64. Official statistics for Madrid show that both groups have roughly equal numbers (999,195 and 996,371 people, respectively, at the beginning of 2024). This difference underscores the added value of this methodology for distinguishing the impact of UAM operations on different population groups depending on where and when they take place.

Figure 2. Duration of noise exceeding 5 dB produced by the cruise flight.

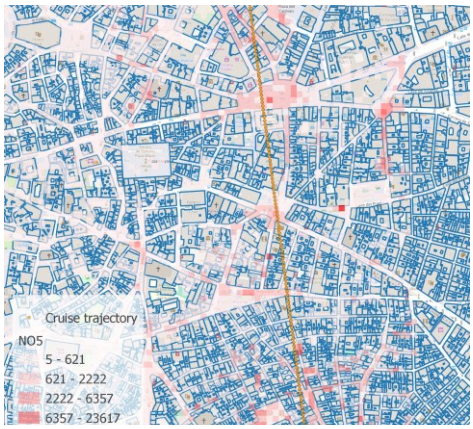

TABLE II. NO5 SEGMENTATION - CRUISE FLIGHT

	Age groups				
Gender	**0-24**	**25-44**	**45-64**	**>65**	**Total**
Female	264 214	418 137	314 046	286 384	1 282 780
Male	232 241	511 966	438 575	190 017	1 372 799
Total	496 455	930 103	752 621	476 401	2 655 579

2) Visual pollution

Fig. 4 displays the visual pollution concentration maps for the drone as it flies over one of the main streets of the city, Gran Vía. These maps reveal that the affected area is consistent, but the magnitude of the VPC varies due to the different formulas. AiRMOUR's metric provides values ranging from 0 to 2, while the visible area affected ranges from 0 to 0.03. Both metrics effectively demonstrate a similar decrease with distance, as expected. In AiRMOUR, this relationship is explicitly included in formula (2), while for the visible area, it is represented by the reduction in the area covered by the drone. As noted in the methodology, the visual pollution concentration takes into account shadowed areas where the drone is not visible. This effect is observable behind buildings, where visibility is restricted. For example, note the cutoffs on the left side of the image where the drone's visibility is obstructed by the building corners on this main street.

Fig. 5 shows the results for the VP1 indicator, which represents the number of people exposed to a single drone operation or, in other words, the number of people who are able to see the drone. The areas with higher numbers of affected people are marked in red on the map.

The distribution of these spots depends on the population distribution itself, so a higher concentration is not necessarily found directly below the drone's trajectory. However, it is more

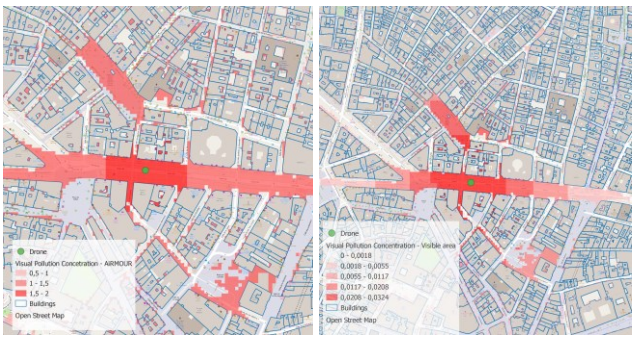

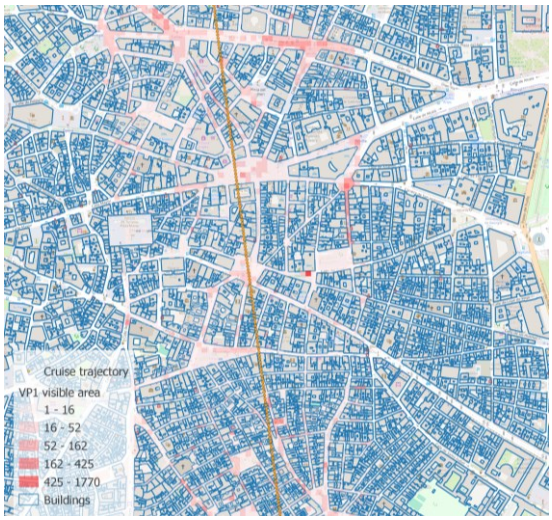

Figure 5. VP1, number of people affected by the flight.

likely that the visible area is concentrated near the drone's flight path, with fewer visible areas and more shadows as distance from the flight path increases. The same segmentation is provided as before, by gender and age groups, in TABLE III. According to the data, a total of 45,125 people would be affected by the drone's presence in the sky. This metric represents an upper limit for the visual impact, as it does not consider the proximity to the drone or a minimum threshold to determine which individuals are actually negatively affected by the drone's visibility.

TABLE III. VP1 SEGMENTATION CRUISE FLIGHT

	Age groups				
Gender	**0-24**	**25-44**	**45-64**	**>65**	**Total**
Female	3 955	6 051	4 635	4 343	18 983
Male	3 479	7 825	6 667	2 798	20 769
Total	7 433	13 876	11 303	7 141	45 125

Fig. 6 presents the results for the VP2 indicator with the VPC based on visible area (the map considering AiRMOUR's VPC is virtually identical). The VP2 indicator shows the number of people affected based on a defined threshold. For the visible area VPC, the threshold is $\pi/100$, while for AiRMOUR it is 0.9, with both thresholds selected to yield similar affected areas.

Despite the very low exposure thresholds chosen for visual pollution concentration, the number of affected people decreases significantly compared to the VP1 results, with a total of 750 people affected according to AiRMOUR's metric and 659 people affected using the visible area metric.

TABLE IV. shows the differences in the affected population depending on the selected threshold for each of the VPC metrics. The threshold for the VPC based on the visible area is more restrictive in this case, excluding 91 people from the metric. It is important to note that these thresholds are configurable, allowing for adjustment of the restriction level.

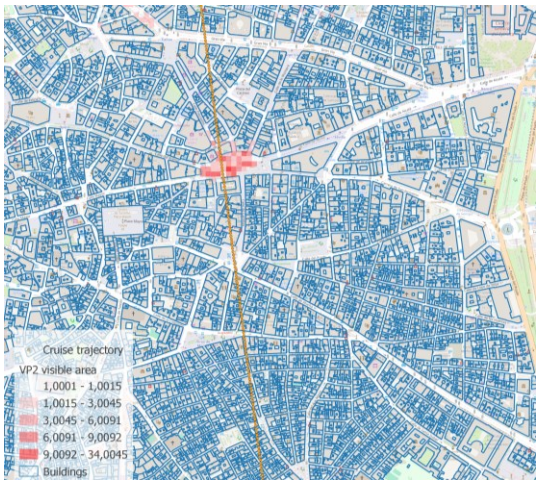

Figure 6. VP2, number of people affected by the flight for a VPC threshold $\pi/100$.

TABLE IV. VP2 SEGMENTATION CRUISE FLIGHT

	Age groups				
Metric / gender	**0-24**	**25-44**	**45-64**	**>65**	**Total**
AiRMOUR	0	91	511	147	750
Female	0	91	256	0	347
Male	0	0	255	147	402
Visible area	0	0	511	147	659
Female	0	0	256	0	256
Male	0	0	255	147	402

Unlike the previous indicators, VP4 not only indicates the number of people affected, but also provides a comprehensive measure of exposure, accounting for both the severity of visual pollution concentration and the duration of exposure for the affected population. Fig. 7 shows that higher VP4 values are concentrated along the trajectory, where visual pollution levels are higher. Additionally, high values are observed in areas with larger populations or where people are exposed for longer periods.

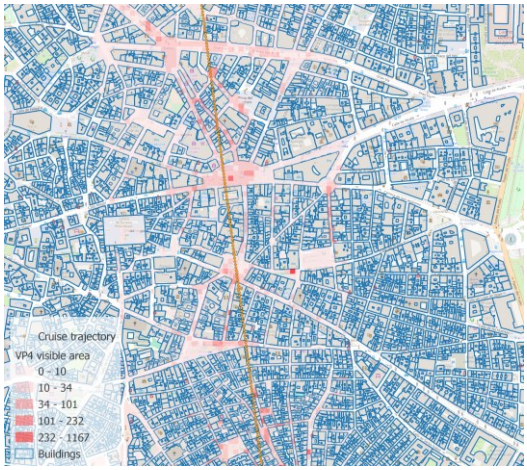

Figure 7. VP4, visual pollution exposure perceived by the people exposed to the flight, [person.vp.h].

TABLE V. shows again the segmentation of the results by age group and gender, considering the two VPC metrics.

TABLE V. VP4 SEGMENTATION CRUISE FLIGHT

	Age groups				
Metric / gender	**0-24**	**25-44**	**45-64**	**>65**	**Total**
AiRMOUR	893 583	1 793 079	1 470 031	898 263	5 740 002
Female	495 469	749 823	616 352	557 364	2 419 009
Male	398 114	1 043 256	853 679	340 899	2 635 948
Visible area	4 322	8 989	7 725	4 435	28 568
Female	2 463	3 459	3 123	2 813	11 858
Male	1 859	5 530	4 601	1 622	13 612

B. *Take-off flight*

1) *Noise*

Fig. 8 shows the equivalent noise level map in dBA over 15 min, produced by a single take-off flight. This calculation, again, serves for illustration purposes only. Single missions should be preferably evaluated through the SEL noise metric included in NO3 [18]. The time duration of integration for the NO1 metric can and will be adjusted in future iterations.

Fig. 9 shows the number of people affected by a noise level greater than 1 dBA, based on the previous data. It is evident that the affected population is concentrated near the flight path, with no impact beyond 200 meters.

Figure 8. Equivalent noise level map (dBA) produced by take-off flight.

Based on the noise and population presence data, it is estimated that a total of 9,430 people are affected by the noise from this flight. Again, the reader should note that the dB threshold used is extremely low, for the same reasons previously explained. Additionally, in the future this calculation will be refined to account for background noise, primarily from road traffic. The Madrid City Council provides strategic noise maps, which will be used to assess whether the noise will be significant at different times of the day (morning, afternoon, and night).

2) *Visual pollution*

Fig. 10 presents the results for the VP1 indicator, which represents the number of people exposed to a single drone operation during take-off. It can be observed that the affected population is concentrated around the flight path as well as in a southern area with higher population density. According to these results, a total number of 17,031 people are able to see the flight.

Fig. 11 illustrates again the VPC values for both metrics considered. In this case, where the flight is taking off, the AiRMOUR metric reaches a value of 3, which is 1.5 times higher than in the previous case of cruising flight, while the visible area metric reaches 0.183, six times higher than in the cruise case. Due to the difference in altitude, the visible area metric is significantly affected by the drone's proximity to the observer. Although not tested in this study, based on VPC equations (1) and (2), the visible area metric would also increase for larger drones, such as air taxis, which occupy a larger visible area for the observer. This effect is not considered by the AiRMOUR metric, which accounts for the number of visible drones, regardless of their size.

Figure 10. VP1, number of people affected by the flight.

Figure 11. Visual pollution maps at an instant of the flight at 65m from

Finally, Fig. 12 shows the VP4 indicator, which measures the total visual pollution exposure. As expected from the VPC maps, the highest values are concentrated around the take-off site.

C. *Traffic*

This case combines the cumulative effects of multiple flights, weighted throughout the day according to their respective time periods: day, evening, or night. Fig. 13 displays the maps of the equivalent noise levels (in dBA).

The map in Fig. 13 is used to calculate the number of people exposed to drones without applying a noise level threshold for detecting affected individuals, in order to provide the most conservative results possible.

The effects are combined with those previously presented: the areas with the highest concentration of affected people are in the city's congested areas, such as Gran Vía and its surroundings, which can be found at the top of Fig. 14, as well as around the take-off site, located at the bottom of the image.

The number of affected people can be segmented by age and gender, similar to previous analyses. TABLE VI. summarises the results obtained.

TABLE VI. NO2 SEGMENTATION TRAFFIC CASE

	Age groups				
Gender	**0-24**	**25-44**	**45-64**	**>65**	**Total**
Female	6 515	8 363	8 994	9 412	33 284
Male	7 342	14 047	10 974	3 859	36 222
Total	13 858	22 409	19 968	13 271	69 506

V. CONCLUSIONS

The results presented in this paper show the utility of the proposed methodology for the purpose of understanding the interaction between UAM operations, environmental impacts, and citizens' use of public spaces. The main contribution of the proposed approach is to characterise population exposure to drones' impact in a dynamic and highly disaggregated manner.

Figure 12. VP4, visual pollution exposure perceived by the people exposed to the flight, [person.vp.h].

The population mapping tools provide differentiation per gender and age groups, information which is very difficult or impossible to achieve with other methods. In addition to gender and age, future work could also include other relevant factors such as occupational status, income level, land use, level of urbanisation, or purpose of flying, all of them closely related to public acceptance of drones.

These preliminary results illustrate the potential of the proposed methodology to make more informed decisions when developing U-space regulations aimed at improving citizens' quality of life. The methodology described in this paper is expected to be the basis for a future U-space service aimed at optimising the social and environmental performance of UAM operations. Upcoming work will aim to achieve a functional toolset that enables the analysis of the complete set of case studies envisioned by the MUSE project.

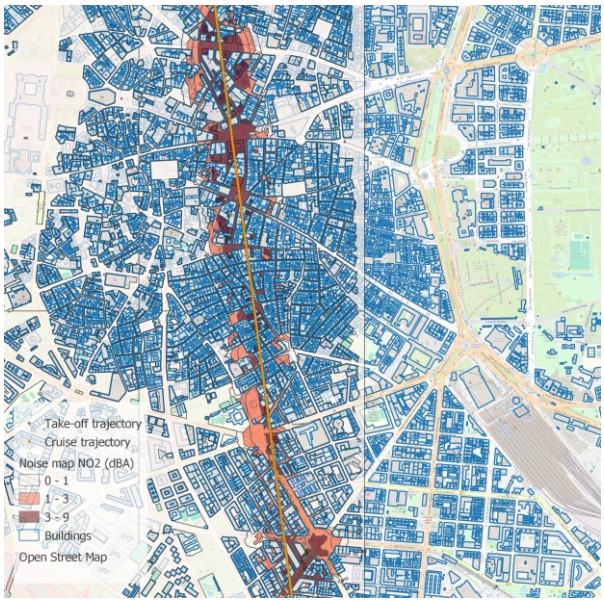

Figure 13. L_{DEN}, Day-evening-night noise level map (24 hours).

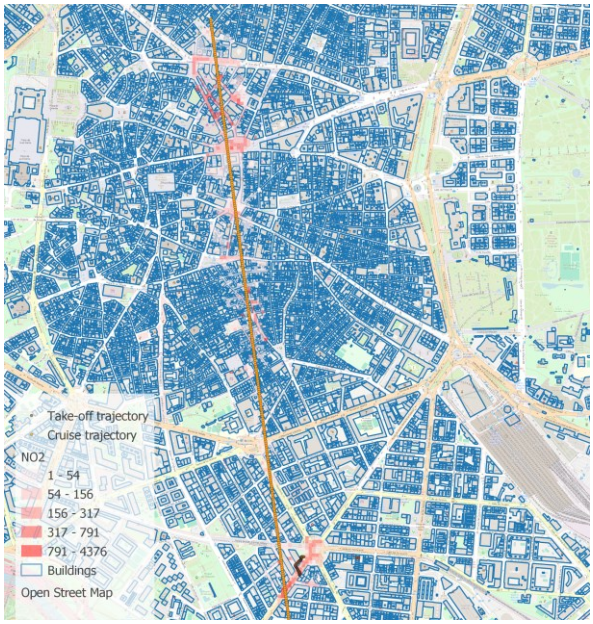

Figure 14. NO2, Area based people exposure to Day-evening-night noise level (L_{DEN}).

ACKNOWLEDGMENT

This research is part of the MUSE project, which has received funding from the SESAR 3 Joint Undertaking (SESAR 3 JU) under grant agreement No 101114858. The JU receives support from the European Union's Horizon Europe research and innovation programme and the SESAR 3 JU members other than the Union. The paper reflects only the authors' view, and that the SESAR 3 JU is not responsible for any use that may be made of the information it contains.

REFERENCES

[1] EASA (2021). Study on the societal acceptance of Urban Air Mobility in Europe.

[2] Biehle, T. (2022). Social Sustainable Urban Air Mobility in Europe. Sustainability, 14(15), 9312.

[3] M. Stolz and T. Laudien, "Assessing Social Acceptance of Urban Air Mobility using Virtual Reality," in 2022 IEEE/AIAA 41st Digital Avionics Systems Conference (DASC), 2022, pp. 1–9.

[4] SESAR PJ19-W2 CI (2023). DES Performance Framework - U-space Companion Document, D4.7.

[5] AiRMOUR project, "D4.3 Noise and visual pollution tools and concepts," Aug. 2023.

[6] Briggs, D., Fecht, D., & De Hoogh, K. (2007). Census data issues for epidemiology and health risk assessment: experiences from the Small Area Health Statistics Unit. Journal of the Royal Statistical Society: Series A (Statistics in Society), 170(2), 355-378.

[7] Baena et al (2024) Measuring U-space Social and Environmental Impact, QuietDrones 2024 September

[8] Barrado, C., Salamí, E., Gallardo, A., Herranz, L. X., & Pastor, E. (2021). Understanding the implications of the future unmanned air traffic growth. In IEEE/AIAA 40th Digital Avionics Systems Conference (DASC).

[9] Hoekstra, J. M., & Ellerbroek, J. (2016, June). Bluesky ATC simulator project: an open data and open source approach. In Proceedings of the 7th international conference on research in air transportation (Vol. 131, p. 132). Washington, DC, USA: FAA/Eurocontrol.

[10] LeGriffon, I. (2019). Noise prediction of a new generation aerostat. In Proceedings of 26th International Congress on Sound and Vibration, ICSV26, Montréal, Canada, 2019.

[11] LeGriffon, I., Bertsch, L., Centracchio, F., & Weintraub, D. (2023, February). Flyover noise evaluation of low-noise technologies applied to a blended wing body aircraft. In INTER-NOISE and NOISE-CON Congress and Conference Proceedings (Vol. 265, No. 6, pp. 1305-1316). Institute of Noise Control Engineering.

[12] European Commission (2015). Commission Directive (EU) 2015/996 of 19 May 2015 establishing common noise assessment methods according to Directive 2002/49/EC of the European Parliament and of the Council, C/2015/3171, OJ L 168, 1.7.2015, p. 1–823.

[13] Bocher, E., Guillaume, G., Picaut, J., Petit, G., & Fortin, N. (2019). Noisemodelling: An open source GIS based tool to produce environmental noise maps. *Isprs international journal of geo-information*, *8*(3), 130.

[14] Chmielewski, S. (2020). Chaos in motion: Measuring visual pollution with tangential view landscape metrics. Land, 9(12), 515.

[15] Nami, P., Jahanbakhsh, P., & Fathalipour, A. (2016). The role and heterogeneity of visual pollution on the quality of urban landscape using GIS; case study: Historical Garden in City of Maraqeh. Open Journal of Geology, 6(1), 20-29.

[16] Romanillos, G., García-Palomares, J. C., Moya-Gómez, B., Gutiérrez, J., Torres, J., López, M., Cantú-Ros, O.G., & Herranz, R. (2021). The city turned off: Urban dynamics during the COVID-19 pandemic based on mobile phone data. Applied Geography, 134, 102524.

[17] Rodr, A. B., Burrieza-Galán, J., Jos, J., de Castro, I. P., Wilby, M. R., & Cantu-Ros, O. G. (2024). Using App Usage Data from Mobile Devices to Improve Activity-based Travel Demand Models. *IEEE Transactions on Big Data*.

[18] MUSE project (2024). D3.1 U-space Environmental and Social Performance Framework.